

Ray dynamics in ocean acoustics

Michael G. Brown

Rosenstiel School of Marine and Atmospheric Science, University of Miami, Miami, Florida 33149

John A. Colosi

Woods Hole Oceanographic Institution, Woods Hole, Massachusetts 02543

Steven Tomsovic

Department of Physics, Washington State University, Pullman, Washington 99164

Anatoly L. Virovlyansky

Institute of Applied Physics, Russian Academy of Science, 6003600 Nizhny Novgorod, Russia

Michael A. Wolfson

Applied Physics Laboratory, University of Washington, Seattle, Washington 98105

George M. Zaslavsky

Courant Institute of Mathematical Sciences, New York University, New York, New York 10012

Recent results relating to ray dynamics in ocean acoustics are reviewed. Attention is focussed on long-range propagation in deep ocean environments. For this class of problems, the ray equations may be simplified by making use of a one-way formulation in which the range variable appears as the independent (time-like) variable. Topics discussed include integrable and nonintegrable ray systems, action-angle variables, nonlinear resonances and the KAM theorem, ray chaos, Lyapunov exponents, predictability, nondegeneracy violation, ray intensity statistics, semiclassical breakdown, wave chaos, and the connection between ray chaos and mode coupling. The Hamiltonian structure of the ray equations plays an important role in all of these topics.

INTRODUCTION

The chaotic dynamics of ray trajectories in ocean acoustics have been explored in a number of recent publications ([1]-[17]). The purpose of the present paper is to provide a review of results relating to this topic. Our exposition is brief but is intended to be self-contained. We introduce a sequence of ray-based simplifications to the mathematical description of underwater sound propagation in order to get a more complete and clear understanding of the underlying propagation physics, especially in range-dependent environments. We consider these simplifications as the starting point of developing a quantitative theory. It is our opinion that even full wave simulations cannot be used effectively without some understanding of the material described in this paper.

To make our discussion more concrete, we focus our attention on long-range propagation in deep ocean conditions. Theoretical results are emphasized, but with an eye toward analyzing measurements. For this reason considerable attention is paid to results that can be applied in the presence of complicated (nonperiodic) range-dependent ocean structure. In a separate paper many of the results presented and discussed here will be applied to the analysis of a particular data set.

In the next section we review important preliminary material. First, we introduce ray-based solutions to the Helmholtz equation. We then introduce the one-way form of the ray equations and the standard parabolic approximation. Finally, the motion of rays in a range-independent environment is discussed. For this class of problems the ray equations are integrable and the

ray trajectories are most naturally described using action-angle variables. In anticipation of the material that follows, the action-angle formalism is introduced.

Section II focuses on the behavior of rays in range-dependent environments, i.e., on nonintegrable ray systems. The action-angle formalism is used here to introduce nonlinear resonances and the KAM theorem. The notion of ray chaos is discussed, as are Lyapunov exponents. Our discussion of the (well known) limitations on the predictability of isolated chaotic trajectories is complemented by a discussion of the (generally unappreciated) stability of families of chaotic trajectories. Also in this section we discuss the connection between an important condition, known as nondegeneracy, and ray stability.

In section III, we discuss ray intensity statistics and related topics, including the distribution of finite range estimates of Lyapunov exponents. The results presented here were first described in the analysis of an idealized underwater acoustic problem, but have since been encountered in other applications. Problems associated with the important task of connecting ray intensity statistics to finite frequency wavefield intensity statistics are discussed.

In section IV, we provide a more general, but brief, discussion of ‘wave chaos’ – the study of wave systems that, in the ray limit, exhibit chaotic motion. This topic falls slightly outside the bounds of providing a review of ray dynamics, but is too important to omit. Strong results relating to this topic are difficult to obtain. Much of our discussion focusses on the question of whether semiclassical (ray-based) wavefield representations break down at the so-called Ehrenfest range, which scales as $\ln(\bar{f})$ where \bar{f} is the appropriately nondimensionalized wave frequency.

In section V, we describe the connection between ray chaos and mode coupling. This work builds on well-known results on ray-mode duality. The results described here provide a promising means of attacking the wave chaos problem inasmuch as finite frequency effects are built into the modal description of the wavefield.

In the final section, we briefly discuss two issues. First, we discuss the principal shortcoming of our current knowledge – our relatively poor understanding of the wave chaos problem. Second, we discuss the manner in which ideas relating to deterministic chaos complement and/or conflict with more traditional ideas relating to the study of wave propagation in random media.

I. PRELIMINARY RESULTS

This section provides background material that is necessary to understand the material that is presented in the sections that follow. Starting with the Helmholtz equation we introduce the ray equations and their one-way form, the standard parabolic approximation, and the action-angle description of ray motion in range-independent environments.

A. Waves and rays

Fixed-frequency (cw) acoustic wavefields satisfy the Helmholtz equation,

$$\nabla^2 u + \sigma^2 c^{-2}(\mathbf{r})u = 0, \quad (1)$$

where $\sigma = 2\pi f$ is the angular frequency of the wavefield and $c(\mathbf{r})$ is the sound speed. In anticipation of our later focus on describing sound fields generated by a point source in environments in which focusing in the azimuthal direction is assumed to be negligible, we shall assume propagation in two space dimensions with $\mathbf{r} = (z, r)$ where z is depth and r is range. The so-called short wave approximation can be used when

$$\sigma \gg \nabla c, \quad (2)$$

i.e., when the acoustic wavelength $2\pi/k$, where $k = \sigma/c$, is smaller than all length scales that characterize variations in c . Under such conditions the solution to (1) can be written as a sum of terms, each representing a locally plane wave,

$$u(\mathbf{r}; \sigma) = \sum_j A_j(\mathbf{r}) e^{i\sigma T_j(\mathbf{r})}. \quad (3)$$

Substitution of the geometric ansatz (3) into the Helmholtz equation (1) gives, after collecting terms in descending powers of σ , the eikonal equation,

$$(\nabla T)^2 = c^{-2}, \quad (4)$$

and the transport equation,

$$\nabla(A^2 \nabla T) = 0. \quad (5)$$

For notational simplicity we have dropped the subscript j on T and A in (4) and (5). The solution to (4) can be reduced to the solution to the ray equations,

$$\frac{d\mathbf{r}}{d\tau} = \frac{\partial \mathcal{H}}{\partial \mathbf{p}}, \quad \frac{d\mathbf{p}}{d\tau} = -\frac{\partial \mathcal{H}}{\partial \mathbf{r}}, \quad (6)$$

and

$$\frac{dT}{d\tau} = \mathcal{L} = \mathbf{p} \cdot \frac{d\mathbf{r}}{d\tau} - \mathcal{H} \quad (7)$$

where $\mathbf{p} = \nabla T$ is the ray slowness (also referred to as the momentum) vector and

$$\mathcal{H}(\mathbf{p}, \mathbf{r}) = \frac{1}{2} (\mathbf{p}^2 - c^{-2}(\mathbf{r})) = 0. \quad (8)$$

The independent (time-like) variable τ satisfies $d\tau/dl = c$ where $dl = |d\mathbf{r}|$, and $d\mathcal{H}/d\tau = 0$. The sum in (3) is over all ray paths $z(r)$ that connect the source at $(z_0, 0)$ and the receiver at (z, r) . The ray equations (6-8) are seen to have Hamiltonian form, which allows many well known results to be applied to the acoustic problem in the short wave limit. Equations (6-8) describe the so-called optical-mechanical analogy of wave propagation in the short wave limit.

For guided wave propagation in the direction of increasing r , the variable r can be used as the independent (time-like) variable and equations (6 - 8) may be rewritten

$$\frac{dz}{dr} = \frac{\partial H}{\partial p}, \quad \frac{dp}{dr} = -\frac{\partial H}{\partial z}, \quad (9)$$

and

$$\frac{dT}{dr} = L = p \frac{dz}{dr} - H \quad (10)$$

where $p = \partial T / \partial z$ is the z -component of the slowness vector,

$$H(p, z, r) = -\sqrt{c^{-2}(z, r) - p^2} \quad (11)$$

is minus the r -component of the slowness vector, and $dH/dr = \partial H / \partial r$. These are the so-called one-way ray equations. All subsequent analysis is based on these equations (or a parabolic approximation to these equations, as described below), rather than the slightly more general equations (6 - 8). Ray angles are defined by the condition $dz/dr = \tan \varphi$ where φ is measured relative to the horizontal. Using (9) and (11) this reduces to $cp = \sin \varphi$. An immediate consequence of equations (9), independent of the form of $H(p, z, r)$, is $\partial(dz/dr) / \partial z + \partial(dp/dr) / \partial p = 0$. This is a statement of

Liouville's theorem, expressing the incompressibility of flow in phase space (p, z) . The one-way ray equations (9) have the same form as the equations describing the motion of a relativistic particle with mass c^{-1} and Hamiltonian H .

The transport equation (5) can be reduced to a statement of constancy of energy flux in ray tubes. In a notation appropriate for use with the one-way ray equations, the solution to the transport equation, assuming a point source, for the j -th eigenray can be written

$$A_j(z, r) = A_{0j} |q_{21}|_j^{-1/2} e^{-i\mu_j \frac{\pi}{2}}. \quad (12)$$

The matrix element q_{21} , defined below, describes the spreading of an infinitesimal ray bundle. At any fixed r , one has

$$\begin{pmatrix} \delta p \\ \delta z \end{pmatrix} = Q \begin{pmatrix} \delta p_0 \\ \delta z_0 \end{pmatrix}, \quad (13)$$

where the stability matrix

$$Q = \begin{pmatrix} q_{11} & q_{12} \\ q_{21} & q_{22} \end{pmatrix} = \begin{pmatrix} \left. \frac{\partial p}{\partial p_0} \right|_{z_0} & \left. \frac{\partial p}{\partial z_0} \right|_{p_0} \\ \left. \frac{\partial z}{\partial p_0} \right|_{z_0} & \left. \frac{\partial z}{\partial z_0} \right|_{p_0} \end{pmatrix}. \quad (14)$$

Elements of this matrix evolve according to

$$\frac{d}{dr} Q = K Q \quad (15)$$

where Q at $r = 0$ is the identity matrix, and

$$K = \begin{pmatrix} -\frac{\partial^2 H}{\partial z \partial p} & -\frac{\partial^2 H}{\partial z^2} \\ \frac{\partial^2 H}{\partial p^2} & \frac{\partial^2 H}{\partial z \partial p} \end{pmatrix}. \quad (16)$$

At caustics q_{21} vanishes and the Maslov index μ advances by one unit. (For waves propagating in three space dimensions, advances by two units are possible.) At these points diffractive corrections to (12) must be applied. The normalization factor A_{0j} is chosen in such a way that close to the source (12) matches the Green's function for the corresponding wave equation, (1) or a parabolic approximation to the one-way form of this equation. (A_{0j} is different for Helmholtz equation and parabolic equation rays; this small difference is of no consequence in the discussion that follows.)

B. The parabolic approximation

The standard parabolic wave equation is

$$-\frac{i}{k_0} \frac{\partial \Psi}{\partial r} = \left(\frac{1}{2k_0^2} \frac{\partial^2}{\partial z^2} - c_0 U(z, r) \right) \Psi \quad (17)$$

where $u(z, r) \approx \exp(ik_0 r) \Psi(z, r)$, $k_0 = \sigma/c_0$,

$$U(z, r) = \frac{1}{2c_0} \left(1 - \frac{c_0^2}{c^2(z, r)} \right), \quad (18)$$

and c_0 is a reference sound speed. The corresponding ray equations are (9) and (10) with $H(p, z, r)$ replaced by

$$H_{PE}(p, z, r) = \frac{c_0}{2} p^2 + U(z, r). \quad (19)$$

Ray angles satisfy $c_0 p = \tan \varphi$. The parabolic approximation is valid when ray angles are small and deviations of $c(z, r)$ from c_0 are small. The parabolic wave equation (17) coincides with the Schrödinger equation with r playing the role of time and k_0^{-1} playing the role of Planck's constant \hbar . It is useful to note this analogy because many tools that have been developed to study quantum chaos, discussed below, can be applied to the study of solutions of (17) or (1) under conditions in which the ray equations, (9) or (6), admit chaotic solutions. In this regard it is noteworthy that there is no quantum mechanical counterpart to transient sound fields as these are characterized by the simultaneous presence of a continuum of k_0 values.

C. Integrable ray systems

It is well known that when the sound speed is a function of depth only and the ocean boundaries are surfaces of constant z , the Helmholtz equation (and the parabolic wave equation) admit separable solutions. Under the same conditions the ray equations also admit simple solutions that make use of action-angle variables, and are said to be integrable. The action-angle formalism is important in the material in much of the remainder of the paper, so the essential results are presented here.

When the sound speed is a function of depth only, ray trajectories are periodic; the ray equations (9) can be transformed, via a canonical transformation, to a new set of ray equations in which the Hamiltonian $H(I)$ is a function of the new momentum variable I but is independent of the new generalized coordinate θ . In terms of the action-angle variables (I, θ) , ray trajectories are described by the equations

$$\frac{d\theta}{dr} = \frac{\partial H}{\partial I} \equiv \omega(I), \quad \frac{dI}{dr} = -\frac{\partial H}{\partial \theta} = 0. \quad (20)$$

The solution to these equations is simply $I = \text{constant}$, $\theta(r) = \omega(I)r + \theta(0)$. These equations (and their higher dimensional counterparts) describe motion on a torus. The action variable can be written (see, e.g., Ref. [18]) as a function of H (which is constant following each ray trajectory in a range-independent environment),

$$I = \frac{1}{2\pi} \oint dz p(H, z) = \frac{1}{\pi} \int_{\hat{z}(H)}^{\hat{z}(H)} dz p(H, z). \quad (21)$$

The integration is over one cycle of the periodic ray trajectory, and at the turning depths $c^{-1}(\hat{z}(H)) = c^{-1}(\hat{z}(H)) = -H$. The generating function for the canonical transformation from (p, z) to (I, θ) is

$$G(z, I) = \int^z dz' p(H(I), z') \quad (22)$$

where the $H(I)$ can be obtained by inverting equation (21), $p = \partial G(z, I)/\partial z$, and $\theta = \partial G(z, I)/\partial I$.

II. NONINTEGRABLE RAY SYSTEMS

Realistic ocean structure is range-dependent, and the corresponding ray systems are nonintegrable. Thus, from a practical point of view, one is forced to consider nonintegrable ray systems. Also, from a more abstract dynamical systems viewpoint, the property of integrability (separable solutions) is known to be rather special. It is now customary to consider nonintegrable systems as being 'generic'. In other words, if an 'arbitrary' set of governing equations of motion were considered, it would most likely be nonintegrable. Only under rare circumstances would a system be found to be integrable. The other end of the dynamical spectrum is the completely chaotic system which is discussed in more detail ahead. Another possibility includes near-integrable dynamics, so-called

because perturbation theory on the nearby integrable system would be valid. Finally, there is mixed dynamics in which both regular and chaotic motion simultaneously exist in the system that are accessed via different initial conditions. Models of ray dynamics in long-range ocean acoustic propagation tend to be in the mixed to fully chaotic regimes.

A. Nonlinear resonances and the KAM theorem

Consider ray motion in an environment consisting of a range-independent sound speed profile to which a small range-dependent perturbation is added. Because of the smallness of the sound speed perturbation, the perturbation to H may be assumed to be additive,

$$H(p, z, r) = H_0(p, z) + \varepsilon H_1(p, z, r). \quad (23)$$

For simplicity, first consider the case where H_1 is a periodic function of r with wavelength $\lambda = 2\pi/\Omega$. It is well known (see, e.g., Ref. [4]) that for this class of problems canonical perturbation theory fails as nonlinear ray-medium resonances are excited for those rays whose action values I_0 in the unperturbed environment satisfy the condition

$$l\omega(I_0) = m\Omega \quad (24)$$

for any pair of integers, l and m .

A simple analysis (see, for example, Ref. [4]) shows that action variables of rays captured into the resonance belong to the interval $I - \Delta I_{\max} < I < I + \Delta I_{\max}$ with

$$\Delta I_{\max} = 2\sqrt{\varepsilon \bar{H}_1 / |\omega'|}, \quad (25)$$

where $\omega' = d\omega(I)/dI$ at $I = I_0$, and \bar{H}_1 is a measure of the magnitude of H_1 . The quantity ΔI_{\max} represents the width of the resonance in terms of the action variable. The width of the resonance in terms of spatial frequency can be approximately estimated as

$$\Delta\omega = |\omega'| \Delta I_{\max} / 2 = \sqrt{\varepsilon \bar{H}_1} |\omega'|. \quad (26)$$

The phenomenon of nonlinear ray medium resonance plays an important role in the emergence of ray chaos. If there are at least two nonlinear resonances centered at spatial frequencies ω and $\omega + \delta\omega$, chaotic motion, according to Chirikov's criterion ([19]-[21]), takes place when the condition

$$\frac{\Delta\omega}{\delta\omega} > 1 \quad (27)$$

is satisfied, i.e., when the resonances overlap leading to the stochastic instability of the system.

One might expect that, even for very small ε , all rays are captured into a nearby resonance. This turns out not to be the case. According to the KAM theorem (see, e.g., Ref. [22]), for sufficiently small ε some of the tori of the unperturbed system are preserved in the perturbed system, albeit in a slightly distorted form. A condition for the applicability of the KAM theorem is that the nondegeneracy condition $\omega' \neq 0$ must be satisfied. This condition guarantees that resonances are isolated provided ε is sufficiently small. Nondegeneracy violation will be discussed in more detail below.

Because realistic sound speed structure in the ocean does not have periodic range-dependence it is important to consider a larger class of perturbation terms $H_1(p, z, r)$. In Ref. [23] it is shown that the KAM theorem applies to problems for which the perturbation term H_1 consists of a

superposition of N components, each of which is periodic in range. N is assumed to be finite but is otherwise unrestricted. The spatial periods need not be commensurable and there may be depth structure associated with each periodic component. Realistic ocean sound speed structure – internal-wave-induced perturbations [24], for example – can be described by a model of this type. A consequence is that the mixture of chaotic and regular trajectories (discussed below) that characterizes ray motion in environments with periodic range-dependence applies to a much larger – and more oceanographically realistic – class of problems.

We note that there is a strong reason to study ray motion in periodic environments even if they seem somewhat unrealistic. In such environments phase space structure can be observed by plotting pairs of points (p, z) at integer multiples of the wavelength λ of the perturbation. Such a Poincaré map, which is found numerically, is a slice of the ray motion in $(p, z, r \bmod \lambda)$. In spite of the artificial nature of the periodicity, the main features found are expected to be qualitatively just like those found with aperiodic environments given that the KAM theorem is equally valid whether the environment has the property $c(z, r + \lambda) = c(z, r)$ for some λ or not.

For some special problems ray dynamics and associated phase space structures can be studied using an even simpler technique which eliminates the need to numerically trace rays. An example is described in Ref. [5]. Here, ray motion in a bilinear model (constant sound speed gradient above and below the sound channel axis) of the deep ocean sound channel was considered. It was shown that when the upper ocean sound speed gradient oscillates periodically in range, successive (separated by one ray cycle) iterates of axial ray angle and range satisfy

$$\begin{aligned}\phi_{n+1} &= \phi_n + \varepsilon[\sin \rho_n + \sin(\rho_n + \phi_n + \varepsilon \sin \rho_n)], \\ \rho_{n+1} &= \rho_n + \phi_n + \varepsilon \sin \rho_n + \gamma \phi_{n+1}.\end{aligned}\tag{28}$$

Here ε is the dimensionless perturbation strength, γ is the ratio of the average upper ocean sound speed gradient g to the fixed lower ocean sound speed gradient, $\phi_n = (4\pi/g\lambda)\varphi_n$ and $\rho_n = (2\pi/\lambda)r_n$. These equations define an area-preserving mapping, $\partial(\phi_{n+1}, \rho_{n+1})/\partial(\phi_n, \rho_n) = 1$; this condition is a discrete analog of Liouville’s theorem. Because of their relative simplicity, area-preserving mappings are widely used to study properties of nonintegrable Hamiltonian systems. Some of these properties will now be described.

B. Ray chaos

Figure 1(a) shows iterates of equation (28) for many sets of ray initial conditions in an environment with moderately strong ($\varepsilon = 0.15$) range-dependence. Phase space is seen to consist of a mixture of regular and chaotic regions, often described as regular islands in a chaotic sea. For much smaller values of ε , chaotic regions occupy only thin isolated bands of phase space. Each such thin chaotic band is associated with an isolated resonance. As ε is increased, the widths of the resonances increase and nearby resonances overlap leading to an intricate mixture of regular and chaotic regions, as seen in Fig. 1(a). Behavior of this type is typical of systems that are constrained by KAM theory. Figure 1(b) shows a plot of range vs. launch angle after 250 ray cycles in the same environment, and using rays emanating from the same fixed point that was used to produce Fig. 1(a). The ray initial conditions used in both Figs. 1(a) and 1(b) fall on a horizontal line (at $r = \lambda/2$) through the middle of Fig. 1(a). Note that the islands that intersect this line in Fig. 1(a) are readily identifiable in Fig. 1(b). This observation is significant because plots like Fig. 1(b) – ray position vs. some continuous ray label – can be constructed in environments with nonperiodic range-dependence, providing a simple means of identifying island-like structures. At the boundaries of chaotic and regular domains – in Fig. 1(a), for example – are usually invisible cantori. These

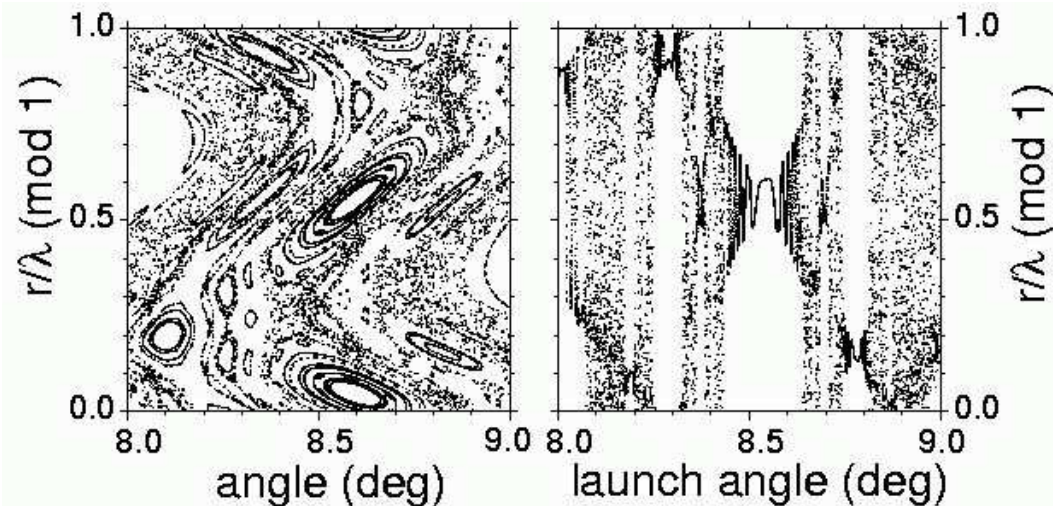


Figure 1: Numerical simulations based on the area-preserving mapping (28) with $g = 1/(30 \text{ km})$, $\lambda = 10 \text{ km}$, $\gamma = 4$ and $\varepsilon = 0.15$. In both plots the ray initial conditions correspond to those of an axial point source at $r = \lambda/2$. Left panel: 500 iterates of the mapping for 50 rays whose launch angles are uniformly distributed between 8 and 9 degrees. Right panel: range after 250 ray cycles (each corresponding to one iteration of the mapping) for 10,000 rays whose launch angles are uniformly distributed between 8 and 9 degrees. In most regions this sampling interval is too large to resolve what should be a smooth function.

are Cantor-type invariant sets with fractal structure containing an infinity of holes. Cantori act as partial barriers that inhibit the diffusion of rays. Boundaries of chaotic regions contain small island chains around which the density of points is very high. A common phenomenon is “stickiness” of island boundaries; after wandering in an apparently random fashion in phase space, a chaotic trajectory may approach a stable island, and stick to its border for some (possibly long) time, during which it exhibits almost regular behavior [25]. The presence of regular islands in phase space alters the dispersion characteristics of the trajectories that lie in the surrounding chaotic sea [25]. Details depend on the structure of phase space but the phenomenon of anomalous diffusion (mean square displacements of trajectories in phase space obeying scaling laws different than that of a traditional random walk) seems to be generic.

An important property of chaotic trajectories is that they exhibit extreme sensitivity, characterized by a positive Lyapunov exponent,

$$\nu_L = \lim_{r \rightarrow \infty} \left(\frac{1}{r} \lim_{\mathcal{D}(0) \rightarrow 0} \ln \frac{\mathcal{D}(r)}{\mathcal{D}(0)} \right). \quad (29)$$

Here $\mathcal{D}(r)$ is a measure of the separation between rays at range r . A closely related quantity is the Kolmogorov-Sinai entropy h_{KS} . Loosely speaking, h_{KS} is a measure of information increase following a trajectory; a readable discussion of this topic can be found in Ref. [26]. For bounded dynamical systems $h_{KS} \sim \nu_L$ holds; in open diffusive systems, their difference is proportional to a diffusion constant [27]. A consequence of the extreme sensitivity of chaotic rays is that the number of eigenrays connecting a fixed source and receiver grows exponentially, like $\exp(h_{KS}r)$, on average in range [1, 9, 12]. Also, the magnitudes of the variational quantities q_{ij} (see equation 14) can

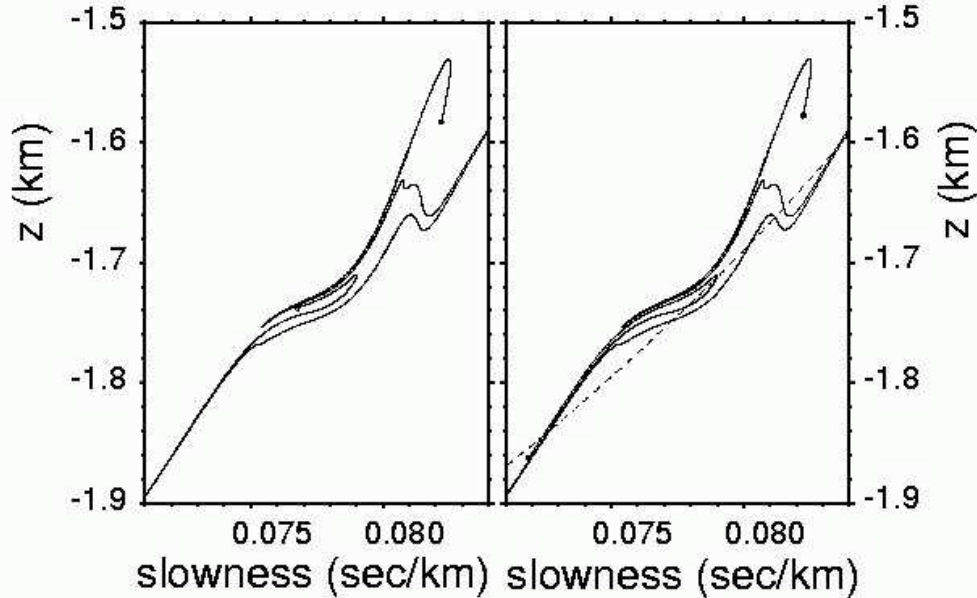


Figure 2: Left panel: segment of a Lagrangian manifold for a fan of rays with $z(0) = -1.100$ km, $8.575^\circ \leq \theta(0) \leq 8.625^\circ$ at $r = 500$ km in the background environment shown in Fig. 3 with an internal-wave-induced sound speed perturbation superimposed. Right panel: segment of a Lagrangian manifold for a fan of rays with $z(0) = -1.101$ km, $8.575^\circ \leq \theta(0) \leq 8.625^\circ$ at $r = 500$ km in the same environment. The endpoints of both Lagrangian manifolds are marked with small open circles. In both panels, portions of the manifold segments, consisting of long thin tendrils, extend beyond the plot boundaries. The dashed curve in the right panel is a portion of a surface $I = \text{constant}$.

grow exponentially, on average, in range. Reference [17] contains a detailed discussion of this topic. A consequence of this exponential growth is that the amplitudes of chaotic rays (proportional to $|\partial z(r)/\partial p(0)|^{-1/2}$ for (9) or $|\partial \rho_n/\partial \phi_0|^{-1/2}$ for (28), assuming a point source) decay exponentially, on average, in range. Note, however, that for moderate to large r or n (measured in units of a typical value of ν_L^{-1}), plots of $\partial z(r)/\partial p(0)$ vs. $p(0)$ (see Fig. 5) or $\partial \rho_n/\partial \phi_0$ vs. ϕ_0 (see Fig. 1) have fractal-like structure when both chaotic and regular trajectories are present.

Another consequence of extreme sensitivity of chaotic rays is that deterministic predictions using finite precision numerical arithmetic is limited to ranges less than some threshold (which is proportional to N_b/ν_L where N_b is the number of bits used to specify the mantissa of floating point numbers). This limitation on one's ability to make deterministic predictions of chaotic ray trajectories at long range is tempered by two related factors. First, the shadowing lemma [26] guarantees that, for a large class of problems, numerically computed chaotic trajectories at long range correspond to trajectories of rays whose initial conditions are close to the specified values but are generally unknown. Second, it is easy to verify that statistical properties of discretely sampled distributions of chaotic rays (occupying, for example, a small but finite area in phase space at $r = 0$) evolve in a way that does not exhibit extreme sensitivity.

A somewhat stronger form of stability of distributions of chaotic rays is illustrated in Fig 2. In phase space an aperture-limited compact source is represented as a line segment at constant depth $z = z_0$ bounded by limiting values of p_0 ; this is an example of a Lagrangian manifold. Each

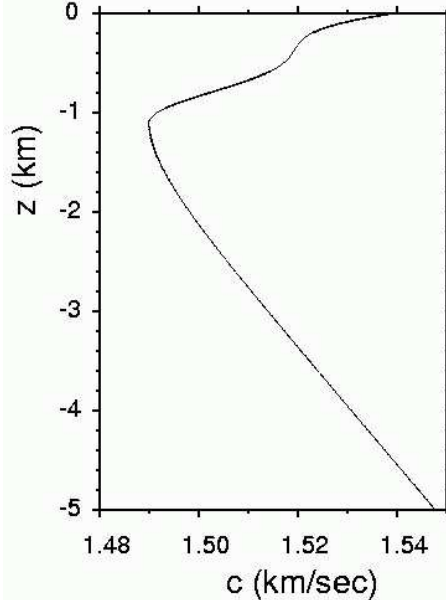


Figure 3: Background sound speed profile used to produce Figs. 2, 4 and 5.

point on such a manifold evolves in r according to the ray equations (9). As a Lagrangian manifold evolves, it gets stretched and folded, but does so without breaking or intersecting itself (owing to phase space area preservation). Fig. 2 illustrates one aspect of a phenomenon that can be termed manifold stability. In this figure two Lagrangian manifolds with slightly different initial conditions are plotted in phase space at a fixed range, $r = 500$ km. Each manifold has initial conditions $z = z_0$ (a constant), $8.575^\circ \leq \theta_0 \leq 8.625^\circ$. For one of the manifolds $z_0 = 1.100$ km; for the other $z_0 = 1.101$ km. Both manifolds evolved in the same environment, which is described below. In this environment almost all trajectories evolve chaotically, which leads to exponential growth in range of the length of each manifold. The combination of chaotic ray motion and the small difference in initial manifold depth might lead one to expect that the two manifolds should evolve very differently. Figure 2 shows clearly, however, that they have not. This can be explained by noting that phase space area is preserved. Because of this constraint, the exponential stretching of each manifold is balanced by an exponential contraction of phase space in the transverse direction. This contraction causes the two manifolds to get squeezed closer to one another. Note, however, that, in general, points on the two manifolds with the same value of θ_0 do not lie close to one another. Loosely speaking, the two manifolds have slid relative to one another while being stretched, folded and squeezed toward one another. Trajectories with nearby initial conditions will also be squeezed toward the same locus of points. Thus, although individual trajectories exhibit extreme sensitivity under chaotic conditions, the associated exponential contraction of phase space elements imparts a surprisingly strong form of stability on continuous distributions of trajectories. The impact of manifold stability on wavefield evolution and stability is considered in Ref. [28].

The environment used to produce Fig. 2 is also used in subsequent numerical work. It consists of a range-independent background profile, shown in Fig. 3, on which an internal-wave-induced sound speed perturbation field is superimposed. The background profile is a Munk [31] profile modified in the upper ocean, $c(z) = c_0(1 + \epsilon(\exp \eta - \eta - 1)) + c_u(z)$, with $c_0 = 1.49$ km/s, $\epsilon = 0.0057$, $\eta = (z - z_a)/B$, $B = 1$ km, $z_a = -1.1$ km, and $c_u(z) = \delta \sin^2(\pi(z - z_a)/z_a)$ for $z > z_a$ with

$\delta = 0.018$ km/s. The internal-wave-induced sound speed perturbation was computed using Eq. 19 of Ref. [24] with $y = t = 0$, i.e., a frozen vertical slice of the internal wave field was assumed. An exponential buoyancy frequency $N(z) = N_0 \exp(z/B)$ (note that depths z are negative with $z = 0$ at the sea surface) with $N_0 = 6$ cycles/hour was used. The dimensionless strength parameters E and μ were taken to be 6.3×10^{-5} and 17.3, respectively. Numerically, a 2^{14} point FFT was used with $\Delta k_x = 2\pi/1638.4$ km, $k_{x,max} = 2\pi/1$ km and $j_{max} = 30$. It should be noted that this perturbation field is highly structured and fairly realistically describes typical deep ocean environments. Also, the assumed background profile is similar to profiles found in much of the North Atlantic Ocean.

We have seen that the generic mixture of chaotic and nonchaotic ray trajectories, the limited predictability of chaotic trajectories, and the strong constraining influence of Liouville's theorem lead to very subtle ray dynamics that blur the distinction between traditional deterministic and stochastic viewpoints. These and related ideas will be further explored in sections that follow.

C. Nondegeneracy violation

Identifying conditions under which the KAM theorem does not apply is important for two reasons. First, inapplicability of KAM theory allows rays to behave chaotically even for infinitesimally small perturbations to the background sound speed structure. Second, the character of this chaotic motion is expected to differ from the chaotic motion of rays constrained by KAM theory. This is because in systems constrained by KAM theory the presence of islands – even small islands – constrains the motion of nearby chaotic trajectories. When KAM theory does not apply, the constraining influence of islands is lost. In this subsection we briefly discuss a cause for KAM theory not to apply – violation of the nondegeneracy condition. We expect that nondegeneracy violation is important in a wide variety of underwater acoustic environments, but the topic has not yet been systematically explored.

Ref. [21] makes a distinction between intrinsic and accidental degeneracy. In the former case $d\omega/dI$ vanishes for all trajectories. Parabolic equation rays in the environment $(c_0/c(z))^2 = 1 - ((z - z_0)/h)^2$ and Helmholtz equation rays in the environment $c(z)/c_0 = \cosh((z - z_0)/h)$ are intrinsically degenerate. These special problems are not realistic oceanographically. Also, it is worth noting that perturbations to intrinsically degenerate systems often break up the degeneracy, leading to phase space structure that is essentially the same as that seen in nondegenerate systems [21]. Accidental degeneracies, on the other hand, occur when $d\omega/dI$ has isolated zeros – when $d\omega/dI$ is plotted as a function of launch angle for a point source, for example. Accidental degeneracies are structurally stable and are fairly common in realistic models of background ocean structure. Thus we expect that accidental degeneracies are important in ocean acoustics. An example of an accidental degeneracy is briefly discussed below.

The foregoing discussion can be quantified somewhat. Recall that two conditions for the validity of KAM theory are: 1) the dimensionless perturbation strength in equation (23) ε is small; and 2) the nondegeneracy condition,

$$\frac{d\omega}{dI} \neq 0 \quad (30)$$

is satisfied in the background environment, which is assumed to be range-independent. Zaslavsky [29] has argued that these conditions may be related; he argued that KAM theory is valid provided

$$\varepsilon < C|\alpha|^\gamma \quad (31)$$

(for small ε and α) for some system-dependent C and $\gamma > 0$ where α is the dimensionless stability

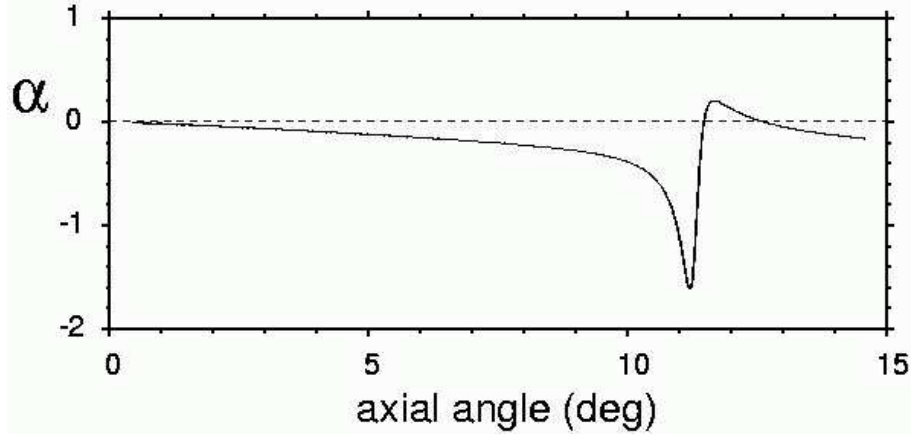


Figure 4: Stability parameter α vs. axial ray angle in the environment shown in Fig. 3.

parameter

$$\alpha = \frac{I}{\omega} \frac{d\omega}{dI}. \quad (32)$$

The term ‘weak chaos’ has been used [30, 6] to describe chaos that is caused by an infinitesimal perturbation to an integrable system. When α vanishes, equation (31) will be violated for arbitrarily small nonzero ε and weak chaos is expected to be present. In Ref. [6] it was demonstrated that rays in a small band surrounding the surface-grazing ray exhibit weak chaos; for the surface grazing ray $d\omega/dI$ – and hence also α – is undefined.

The stability parameter α can be computed from more familiar ray quantities. The angular frequency $\omega = 2\pi/R$ where R is the ray cycle distance. For Helmholtz equation rays

$$R(p_r) = 2p_r \int_{\tilde{z}}^{\hat{z}} \frac{dz}{(c^{-2}(z) - p_r^2)^{1/2}} \quad (33)$$

where p_r is the r -component of the ray slowness vector, which is constant following a ray trajectory in a range-independent environment. The upper turning depth of a ray $\hat{z}(p_r)$ satisfies $c(\hat{z}(p_r)) = p_r^{-1}$, and similarly for the lower turning depth $\tilde{z}(p_r)$. Also, $cp_r = \cos \varphi$. The action can be written

$$I(p_r) = \frac{1}{\pi} \int_{\tilde{z}}^{\hat{z}} dz (c^{-2}(z) - p_r^2)^{1/2}. \quad (34)$$

Because $2\pi dI/dp_r = -R(p_r)$, $\alpha = (2\pi I/R^2)dR/dp_r$. This expression for α is convenient to evaluate numerically.

Figure 4 shows α as a function of axial ray angle in the environment shown in Fig. 3. It is seen that α has two zero crossings for rays with axial angles near 12° . Figure 5 shows a plot of ray depth vs. launch angle for an axial source at a range of 1000 km in this environment with an internal-wave-induced sound speed perturbation superimposed. (The internal-wave-induced perturbation used to produce Fig. 5 is identical to that used to produce Fig. 2 apart from a factor of two reduction in the strength parameter E .) In Fig. 5 it is seen that rays in the 10° to 12° band are evidently much less stable than those outside this band. Outside of this band there is evidence of apparently nonchaotic island-like structures (compare to Fig. 1); inside this band there is no indication – at the resolution shown, at least – of the presence of such structures. We attribute this

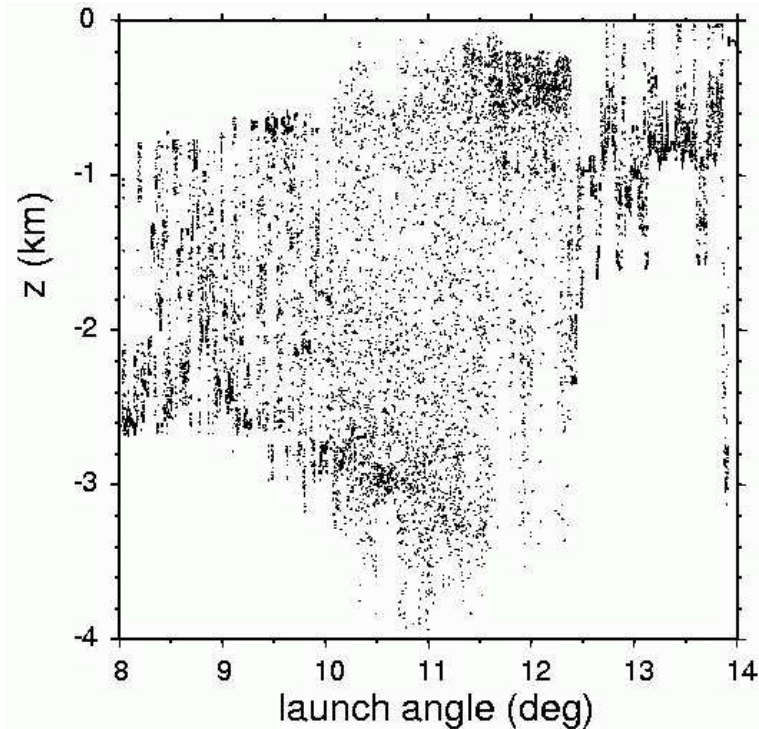


Figure 5: Ray depth vs. launch angle for an axial source at a range of 1000 km in the background environment shown in Fig. 3 with an internal-wave-induced sound speed perturbation superimposed. In most regions the sampling interval ($\Delta\theta_0 = 0.0005^\circ$) is too large to resolve what should be a smooth function.

difference to rays in the more stable regions being constrained by KAM theory. (The slight upward shift of the unstable band of axial ray angles in Fig. 4 relative to Fig. 5 is not unexpected. In the presence of internal waves in the deep ocean, the upper turning depths of rays whose axial angles are more than a few degrees tend to move slightly toward the surface – or equivalently, axial ray angles increase slightly – with increasing range. This is because, following such a ray, scattering is strongest near the ray’s upper turning depth; any perturbation to the ray angle at the upper turning depth will make the ray steeper.)

Because accidental degeneracies are not uncommon in realistic models of (background) ocean structure, we expect the qualitative behavior exhibited in Figs. 4 and 5 to be fairly common in ocean acoustics. The occurrence of accidental degeneracies may be the cause of the finding of Simmen et al. [14] that, for identical sound speed perturbation fields, characteristics of ray stability vs. launch angle curves depend strongly on the background sound speed profile. The connection between nondegeneracy violation and ray stability needs to be further investigated.

III. RAY INTENSITY STATISTICS

Ray intensity distributions are discussed in this section. There are two principal reasons for investigating this topic. First, ray intensity distributions are a useful diagnostic tool to study and quantify ray dynamics, especially in environments with nonperiodic range-dependence where Poincaré maps

cannot be constructed. Second, one expects – on the basis of the local plane wave expansion (3) – that a useful starting point for understanding wavefield intensity statistics is understanding ray intensity statistics. We emphasize that gaining an understanding of ray intensity statistics is only the first step in this process, as diffraction and interference effects must be accounted for in making the transition to wavefield intensity statistics. These complications will be discussed in more detail below.

We shall confine our attention to a discussion of ray intensity statistics in a simple idealized ocean model. A more detailed account of the results presented here can be found in [17]. Some related results for the same idealized problem are presented in [16]. The model consists of an unbounded homogeneous background on which an isotropic, single scale (described by a Gaussian spectrum) random perturbation is superimposed. It should not be expected that all of the properties of ray intensity distributions in our idealized problem carry over to long-range deep ocean propagation conditions, which are characterized by the presence of a background sound channel on which strongly inhomogeneous and isotropic internal-wave-induced sound speed fluctuations with a power-law spectrum are superimposed. In spite of the idealized nature of the problem considered here, there is ample justification for studying this problem. First, this simple problem has surprisingly rich structure that must be understood before more complicated problems can be successfully attacked. Second, the results presented are expected to comprise a limiting case of those that apply to more complicated problems. And third, preliminary results suggest that many of the results presented here apply generally to systems that are far from integrable. This topic will be discussed in more detail elsewhere.

It is also worth mentioning that the results presented here are expected to apply to other fields, as well. Twinkling starlight is a familiar example, but far more exotic systems with the same dynamical foundation exist. Two such examples are the gravitational bending of light passing through galaxy clusters [32], and the quantum mechanical waves associated with low temperature, conduction electron transport through semiconductor materials [33]. Recent experiments of this latter system show the electron transport breaking up into coherent channels that follow bundles of classical rays that are only weakly unstable in spite of the semiconductor acting as a random medium [34]. This is a manifestation of the remaining stable and nearly-stable rays mentioned in Sect. II in connection with the KAM theorem; such rays will show up again later in this section.

Ray stability analysis relies on the stability matrix Q defined in Eq. (13) from which a great deal of information can be deduced. It describes the behavior of all the rays that remain within an infinitesimal neighborhood of a reference ray over the course of its propagation. As seen in Eq. (12), geometric amplitudes for a point source are controlled by the matrix element q_{21} ; for a plane wave initial condition q_{22} is the relevant quantity. For pedagogical purposes, however, it is simpler to consider the trace of the matrix; for chaotic rays, its exponential rate of increase and gross statistical properties are the same as those of any of the Q matrix elements. Since Q is diagonalizable by a linear, similarity transformation

$$\Lambda = LQL^{-1} \implies \begin{pmatrix} \lambda & 0 \\ 0 & \lambda^{-1} \end{pmatrix}, \quad (35)$$

its trace is an invariant equal to the sum of the eigenvalues. The last form applies to systems with a single degree of freedom because the determinant is unity. Three distinct cases may arise. The first is $|\text{Tr}(Q)| < 2$ which is linked to stable motion, and it is customary to denote $\lambda = \exp(i\theta r)$. The second case is $|\text{Tr}(Q)| = 2$, and it is often called marginally stable because it is the boundary case between stable and unstable motion. The third case represents unstable motion, and is characterized by $|\text{Tr}(Q)| > 2$. There it is customary to denote $\lambda = \pm \exp(\nu r)$ where ν is positive and real.

In systems that are far from integrable, the vast majority of rays falls into this last category. Their largest Lyapunov exponent takes on an alternative form to Eq. (29), which can be expressed as

$$\nu_L \equiv \lim_{r \rightarrow \infty} \frac{\ln(|\text{Tr}(Q)|)}{r} . \quad (36)$$

In the limit, $r \rightarrow \infty$, effectively all rays converge to a unique value for ν_L . At finite ranges, each ray has different properties, and it is quite helpful to introduce the concept of a finite range Lyapunov exponent (sometimes known as stability exponent). For unstable orbits, $\text{Tr}(Q) = \lambda + 1/\lambda \approx \lambda$ with little inaccuracy giving

$$\nu = \frac{\ln |\text{Tr}(Q)|}{r} ; \quad (37)$$

if necessary the more precise definition $\nu = \cosh^{-1}[\text{Tr}(Q)/2]/r$ could be used, but it makes little difference for the discussion. Thus, in the limit, ν approaches ν_L for every ray. The relationship between these two exponents is rendered evident by introducing an ensemble of potentials U each of which generates a chaotic dynamical system of fixed ν_L . The ensemble average of ν converges to ν_L without the necessity of the $r \rightarrow \infty$ limit, except at very short ranges.

A very important property of these relations is that even small or modest fluctuations in ν produce immense fluctuations in $\text{Tr}(Q)$ which imply similar fluctuations in q_{21} . Although, long propagation ranges in chaotic systems imply vast numbers of eigenrays, the wave field may be dominated by those far fewer terms that appear in the summation with very small q_{21} .

An analytic expression for the root mean square exponential rate of increase of $\text{Tr}(Q)$ has been derived using techniques relying on Markovian assumptions [16]:

$$\text{Tr}(Q)_{RMS} \sim \exp(\nu' r) . \quad (38)$$

where

$$\nu' \approx \left(\frac{1}{2} \int_0^\infty d\xi \left\langle \frac{\partial^2 U(z; r - \xi)}{\partial z^2} \Big|_{\substack{z=z_0 \\ p=p_0}} \frac{\partial^2 U(z; r)}{\partial z^2} \Big|_{\substack{z=z_0 \\ p=p_0}} \right\rangle \right)^{1/3} , \quad (39)$$

and the brackets, $\langle \dots \rangle$, denote ensemble averaging over different realizations of the potential U . Numerical evaluation of Eq. (39) for model systems with some realism is usually necessary, but analytic results are available for simplified models such as Gaussian random single scale potentials.

Interestingly, ν' is greater than the Lyapunov exponent, independent of the range involved. In fact, with increasing range it rapidly approaches a constant. The important distinction lies in whether the ensemble averaging occurs before or after taking the natural logarithm. The fluctuations are strong enough that $\nu' > \nu_L (= \langle \nu \rangle)$ or alternatively

$$\frac{\ln \langle |\text{Tr}(Q)|^2 \rangle}{2r} > \left\langle \frac{\ln |\text{Tr}(Q)|}{r} \right\rangle \quad (40)$$

for all appreciable r .

It turns out that, for a homogeneous background and single scale Gaussian random medium, to an excellent approximation except in the far tails, the probability density of ν is a Gaussian of mean ν_L and variance

$$\sigma_\nu^2 = \frac{\nu' - \nu_L}{r} . \quad (41)$$

This distribution has also been observed in numerical simulations based on more realistic ocean models. This topic will be discussed in more detail elsewhere. Numerical calculations also suggest

that the Gaussian statistics are obtained for each realization of the random medium just by choosing different initial conditions; i.e. an ensemble of media is not necessary. A Gaussian density for ν implies a lognormal density for $|\text{Tr}(Q)|$ whose parameters are fixed by the Gaussian density's mean and variance. A property of lognormal densities is that any power of the variable also has a lognormal density. Thus, $|\text{Tr}(Q)|^\gamma$ has a lognormal density as well; $\gamma = -1/2$ relates to the semiclassical approximation. However note that depending on the value of γ , the lognormal density may fail as an approximation less far out in the tails.

In the limit of long range, the fluctuations in $|\text{Tr}(Q)|$ grow without bound despite ν approaching ν_L for every ray. Just as there are highly unstable rays, there are also rays which are stable or nearly stable. The lognormal density gives a prediction for what approximate proportion is left for a given propagation range. Asymptotically, the proportion of nearly stable rays, whose stability exponent is less than some small value ν_c , decreases exponentially with range as $(a_0/4\pi r)^{1/2} \exp(-r/a_0)$ where $a_0 = 2(\nu' - \nu_L)/(\nu_L - \nu_c)^2$.

The connection to the statistical behavior of wave field intensities arising from the lognormal density of classical ray intensities is not yet understood. There are a number of subtleties. To begin with, for long ranges of propagation, the most naive picture of semiclassical theory leads to the expectation that the wavefield is made up of an extremely large number of extremely small contributions. On average, if diffusive growth in phase space is neglected, the growth of the number of eigenrays and the decay of a typical ray intensity (squared amplitude) should occur at the same exponential rate. If this is true, energy conservation considerations dictate that at long range the constituent ray arrivals have effectively random phases. In other words, a set of N random, uncorrelated numbers of scale $N^{-1/2}$ maintains an order unity summation as $N \rightarrow \infty$. Chaotic dynamics is deterministic, and at best, the semiclassical phases generated by the dynamics are pseudo-random at long range. For shorter ranges, correlations amongst the magnitudes and phases could alter the statistical predictions. These correlations remain to be studied. Furthermore, the possibility mentioned earlier that one or few very strong terms at short range could dominate the sum increases the difficulty in finding a unique approach to an asymptotic statistical limit.

A second difficulty is that the lognormal distribution has long tails indicative of its broad range of fluctuations. It has the form $y^{-a_0 \ln y}$ which can be verified to approach zero for large or small y faster than any power of y , but does not decay exponentially. A sum of random numbers chosen from long tailed densities may not approach a standard central theorem limit (the Lorentzian density remains Lorentzian under repeated convolution), or may approach it very slowly. For the ray chaos problem, as more and more eigenrays exist with increasing range, the breadth of the density is also increasing. If the approach to a central limit theorem is slow enough, then it might never be reached under these circumstances; the limiting density still needs to be worked out.

A third, extremely important difficulty is the appearance of caustics. Their number proliferates at the same exponential rate for chaotic systems as the number of eigenrays. At the caustics, the semiclassical expressions diverge and introduce infinities. They correspond to the extremely small values of instabilities in the tail of the lognormal density where breakdown of the statistical laws are likely. Thus, the lognormal expression does not, for example, capture the physics of singularity dominated fluctuations that are characterized by twinkling exponents which depend on the types of caustics present [36, 37, 38]. Some incorporation of deviations from lognormality appears to be inescapable. In addition, the presence of exponentially proliferating numbers of caustics calls into question the very relevance of semiclassical methods and their usefulness in predicting the statistical properties of the wave field. This consideration is intimately linked with discussions of the validity of the semiclassical approximation for chaotic systems of which we give an overview in the next section.

A final noteworthy complication arises in the analysis of sound fields produced by a broadband

source. Interference must still be accounted for, but only among ray arrivals whose travel times fall within intervals whose duration is the reciprocal bandwidth $(\Delta f)^{-1}$ of the source. This phenomenon is further complicated when pulse shapes and phase shifts at caustics – corresponding to Hilbert transforms in the time domain – are taken into account. Surprisingly, in spite of the widespread use of broadband sources in ocean acoustic experiments, we are unaware of any attempt to systematically account for all of these complexities in a theory of broadband intensity statistics.

IV. WAVE CHAOS

‘Wave chaos’ is the study of wave systems that, in the ray limit, exhibit unstable dynamics (i.e. exponential divergence of neighboring rays); therefore the ocean acoustics problem can be thought of as a wave chaos problem. A completely analogous definition of the phrase ‘quantum chaos’ is also widely used. These two subjects are similar enough that much, if not most, of the progress in either domain carries readily over into the other; we therefore do not bother to distinguish them here. It turns out that there are significant conceptual difficulties with attempting to associate wave chaos with an unbounded, exponential growth of wavefield complexity in the hope that a straightforward generalization of the underlying ray chaos manifests itself. The shorthand explanation of this difficulty is often crudely stated something like, “the finite wavevector (nonzero Planck’s constant \hbar) smooths over the intricate, fine scale details of the chaotic dynamics, not allowing them to be seen.” The correspondence principle for chaotic systems, in fact, is quite subtle, and we avoid going into this fascinating subject except for the issue of the breakdown of semiclassical theories which we summarize next [39]. For further details though, we refer the reader to Ref. [40] for a discussion of some aspects of wave chaos in underwater acoustics, and to some recent literature relating to quantum chaos [41, 42].

The aspect of the breakdown of semiclassical theories which interests us most for the purposes of this paper is whether or not it is possible to construct, on solid theoretical ground, a ray-based theory valid beyond where ray chaos has fully developed. If not, ray-based predictions under chaotic conditions that match data in long-range propagation experiments would have to be considered accidental, and not an explanation of the essential physics of the problem. It may turn out that the eventual answer to this question is not unique, and depends upon which quantity one wishes to explain. For example, statistical predictions may be more robust than detailed, point-wise, wavefield predictions. On the other hand, if the breakdown occurs on a scale much longer than that of the development of ray chaos, there remains a great deal of theoretical work to be pursued.

There is some hope for optimism in this regard. We begin by distinguishing between two classes of dynamical systems. The first class is that of simple, chaotic systems. Equations (28) define a system of this type. The equations of motion may be deceptively simple to write down, yet the solutions highly complicated, and, for all intents and purposes, analytically intractable (chaotic). The second class has complicated equations in the sense that the medium satisfies many of the criteria of randomness even though it is taken here to be deterministic (we may not know which deterministic realization is given in a particular case). One cannot take for granted the equivalence of the properties of these two classes of systems (chaotic versus random media), but we note that in certain limits there exist a number of common results (such as exponential ray instability with respect to initial conditions).

In simple chaotic systems, about which more is known concerning semiclassical breakdown, we have to be careful to distinguish three levels of dynamics: classical, quantum, and semiclassical. We emphasize that the latter should be distinguished from the classical in that it takes classical information as input, but it actually generates an approximate construction of the quantum dynamics at the level of wave amplitudes and phases. The distinctions between time-evolving classical and

quantum expectation values of operators or classical and quantum probability densities have been studied since the development of quantum mechanics. Those quantities that correspond to each other initially are known to propagate similarly before diverging over a finite time scale called the Ehrenfest time. For simplicity, we shall focus only on the fact that one cannot delay the onset of interference phenomena in the quantum dynamics beyond the Ehrenfest time, and interference is necessarily excluded from the classical dynamics. For chaotic systems, the Ehrenfest time depends logarithmically on \hbar [43], and beyond this time scale one finds all manner of complications such as an exponential proliferation of rays, increasing uncertainty whether the rays can even be calculated, and proliferating caustics in semiclassical theories. There is no debate whether the classical and quantum dynamics diverge beyond the Ehrenfest time (they do by definition); the relevant debate centers upon whether a ray-based, semiclassical theory can surmount these difficulties.

There are various ‘flavors’ of semiclassical approximations possible. For example, the Wigner-Weyl calculus or other constructions of pseudo-phase spaces [44] are ideally suited for exhibiting how the classical limit emerges from quantum mechanics in a semiclassical limit, but they are poorly adapted for describing interference phenomena. Indeed, mathematical proofs exist that such phase-space-based semiclassical approximations cannot be extended beyond a logarithmic time scale; see [45]. In this scenario, it can be fruitful to examine smoothed features of the wave field (as opposed to pointwise comparisons), such as can be obtained through the ray-based construction of the coarse-grained Wigner function [46]. However, the development of semiclassical approaches that can be roughly described as time-dependent WKB theory handle interference naturally through multiple stationary phase (saddle point) contributions. This approach has been applied to a number of paradigms of chaos (the baker’s map, the stadium, and the kicked rotor) with excellent, numerical results extending well beyond the logarithmic time scale [47, 48, 49]. Arguments leading to the expectation that the breakdown time depends algebraically on \hbar have also been presented [48, 49, 50].

Semiclassical breakdown in an idealized, but highly structured, ocean model consisting of a single realization of an ensemble with prescribed statistics has been investigated by Brown and Wolfson. They constructed the full semiclassical approximation using the classical dynamics and a Maslov-Chapman uniformization procedure. In their comparisons, they found the semiclassical approximation appeared to be working quite well beyond the onset of ray chaos [51]. This work and those quoted for simple chaotic systems are claiming that it is possible to extend a semiclassical theory for both chaotic and random media problems beyond a logarithmic time (range) scale, and thus, that ray-based semiclassical theories are viable candidates purporting to explain the essential physics of wave chaotic dynamical problems.

V. CHAOS AND MODE COUPLING

The connection between ray and modal expansions of acoustic wavefields in range-independent environments is well understood (see, e.g., Refs. [52]-[54]) and some generalizations have been derived [55]-[57] for range-dependent environments. Thus, it should come as no surprise that there is a quantifiable connection between ray chaos and the modal description of the wavefield. A detailed description of this connection is described in Refs. [58] and [59]. In this section, the connection between ray chaos and mode coupling is briefly described. To simplify the presentation somewhat, we make use of a WKB analysis of the parabolic wave equation. Consistent with our use of the parabolic wave equation, the variables $p' = c_0 p$, $H' = c_0 H_{PE}$, $U' = c_0 U$ and $I' = c_0 I$ are used in this section after dropping the primes. Also, $S = c_0 T$ is used in place of T .

The principal result of this section is an approximate analytical expression for mode amplitudes in terms of ray-like quantities. We discuss how typical features of ray chaos, such as exponential

growth (with range) of eigenrays contributing to the field point and coexistence of chaotic and regular ray trajectories manifest themselves in the mode amplitude range-dependence. The phenomenon of nonlinear ray-medium resonance that plays a crucial role in the emergence of ray chaos is shown to have an analog for modes which we call the mode-medium resonance [58]. According to the heuristic criterion proposed by Chirikov [19]-[21], chaos is a result of an overlap of different resonances. In terms of normal modes, chaos is shown to result from overlapping mode-medium resonances leading to complicated and irregular range variations of the modal structure.

The normal mode representation of the solution to the parabolic wave equation (17) is obtained by expanding $\Psi(z, r)$ in a sum of eigenfunctions of the unperturbed Sturm-Liouville eigenvalue problem [60, 61],

$$-\frac{1}{2} \frac{d^2 \psi_m}{dz^2} + k_0^2 U_0(z) \psi_m = k_0^2 E_m \psi_m, \quad (42)$$

where ψ_m and E_m are the eigenfunctions and eigenvalues, respectively:

$$\Psi(z, r) = \sum_m B_m(r) \psi_m(z). \quad (43)$$

Here it is assumed that $U(z, r) = U_0(z) + \varepsilon V(z, r)$ and \bar{V} is a measure of the magnitude of V . Each term in the sum (43) represents a contribution from an individual normal mode. In order to get simple semiclassical expressions for the amplitudes, B_m , we project the ray representation of $\Psi(z, r)$ of the form of Eq. (3) onto the normal modes. Assuming the latter to be normalized in such a way that

$$\int_{-\infty}^{\infty} dz \psi_m(z) \psi_n(z) = \delta_{mn}, \quad (44)$$

we need to evaluate the integrals

$$B_m(r) = \int_{-\infty}^{\infty} dz \Psi(z, r) \psi_m(z). \quad (45)$$

Since we consider the geometric approximation to $\Psi(z, r)$, it is natural to use the same approximation for $\psi_m(z)$. The corresponding formulas are usually referred to as the WKB approximations to the eigenfunctions [54, 60, 61].

We shall assume that the potential $U_0(z)$ is smooth, has only one minimum and its walls tend to infinity as $z \rightarrow \pm\infty$. When this assumption is combined with use of the WKB approximation, the eigenvalues of the action variable I_m are determined by the quantization rule

$$k_0 I_m = m + \frac{1}{2}. \quad (46)$$

Then the eigenvalues of the “energy” are given by the relation $E_m = E(I_m)$, where the function $E(I)$ is determined by Eq. (21). In the same approximation the m -th eigenfunction $\psi_m(z)$ between its turning points can be represented as [54, 61]

$$\psi_m(z) = \psi_m^+(z) + \psi_m^-(z), \quad (47)$$

with

$$\psi_m^\pm(z) = Q_m(z) \exp \left[\pm i \left(k_0 \int_{\bar{z}}^z dz' \sqrt{2[E_m - U_0(z')]} - \frac{\pi}{4} \right) \right], \quad (48)$$

$$Q_m(z) = \frac{1}{\sqrt{R_m} [2(E_m - U_0(z))]^{1/4}}, \quad (49)$$

where R_m is the cycle length of the ray in the unperturbed waveguide with $E = E_m$. In this form the eigenfunction is represented as a sum of two terms with rapidly varying phases and slowly varying amplitudes. Substituting Eqs. (47) and the ray representation of $\Psi(z, r)$ of the form (3) into Eq. (45) yields a sum of integrals which can be approximately evaluated by applying the stationary phase technique [54]. This has been done in Ref. [58]. Earlier, a related result was obtained in Ref. [62]. Here we present only the final expressions for B_m .

It turns out that the amplitude of the m -th mode at the given range r is formed by contributions from the rays with action variables equal to that of the given mode, i.e., with

$$I = I_m. \quad (50)$$

Equation (50) singles out a set of rays which we shall call the eigenrays for the m -th mode. The action variable on the left is considered as a function of range, and initial values of the momentum p_0 and the coordinate z_0 , i.e.,

$$I = I(p_0, z_0, r). \quad (51)$$

This function is determined by the solutions to Eqs. (9) and (19), and Eq. (21). For a point source the value of z_0 is the same for all rays; substitution of Eq.(51) into Eq.(50) then yields an equation for p_0 , whose solutions define the initial momenta of the eigenrays contributing to the m -th mode.

The process of identifying modal eigenrays is illustrated in the right panel of Fig. 2. Two curves are plotted: a surface of constant I and a segment of a Lagrangian manifold. The Lagrangian manifold corresponds, at $r = 0$, to a small angular aperture point source. Each intersection of the two curves corresponds to a modal eigenray. Eleven such intersections are shown. Under chaotic conditions this number can grow exponentially in range. (In contrast, in all range-independent environments there are two modal eigenrays for each mode, independent of range, whose launch angles have opposite sign.)

The mode amplitude is given by the sum

$$B_m = \sum_n \frac{1}{\sqrt{k_0 |\partial I / \partial p_0|_{p_0=p_{0n}}}} e^{ik_0 \Phi_n + i\beta_n}, \quad (52)$$

where each term represents a contribution from an eigenray with an initial momentum p_{0n} . The explicit expressions for the phase terms are (since the subsequent formulas describe characteristics of a single eigenray, the subscript n is omitted)

$$\Phi = S - S_0(z, I_m) \operatorname{sgn}(p) \quad (53)$$

and

$$\beta = \left(\operatorname{sgn} \left(\frac{\partial p / \partial p_0}{\partial z / \partial p_0} \right) - \operatorname{sgn}(p) - 2\mu \right) \frac{\pi}{4}. \quad (54)$$

Here z is the depth and p is the momentum of the eigenray at a range r , S and μ are its eikonal and Maslov index, respectively.

Equations (51)-(54) provide the analytical description of mode amplitudes in a range-dependent environment through the parameters of ray trajectories, i.e. through solutions to the Hamilton equations (9). These equations reduce the mode amplitude evaluation to a procedure quite analogous to that generally used when evaluating the field amplitude at the given point. This involves solving the Hamilton (ray) equations, finding the eigenrays, and calculating ray eikonals and some derivatives with respect to initial values of ray parameters. An important point should be stressed.

Although we expand the wavefield over eigenfunctions of the unperturbed waveguide, smallness of the perturbation has not been assumed. Our small parameter is the acoustic wavelength, $2\pi/k$, that should be substantially smaller than any physical scale in the problem.

Having the comparatively simple expressions relating the mode amplitudes to rays, we can now discuss how the complicated ray trajectory dynamics reveals itself in the mode amplitude variations. For simplicity, we restrict our attention to a waveguide with a weak (ε is now considered as a small parameter) periodic range dependence with a spatial period $2\pi/\Omega$, and we consider the case when only one mode is excited at $r = 0$, i.e.

$$u(0, z) = \psi_m(z). \quad (55)$$

Analysis of the ray structure for this type of distributed source (see Refs. [58, 59]) shows that for all rays initial values of the action variable I are equal to I_m . A situation which we call *mode-medium resonance* occurs when the value of I_m satisfies Eq. (24). Due to the resonance, at ranges of order of $1/\Delta\omega$ there will appear a bundle of rays with the action variables I in the interval $|I - I_0| < \Delta I_{\max}$. This means (see Eqs.(50)) that starting with such ranges, the m -th mode is split into a group of $2M$ modes with

$$M = \Delta I_{\max}/k_0 = 2\sqrt{\varepsilon\bar{V}/|\omega'|}/k_0. \quad (56)$$

This expression is the modal analog of the standard expression (Eq. 25) for the width of a ray resonance. In the case of overlapping modal resonances it is natural to expect a further broadening of a group of modes. Moreover, as we discussed earlier, the overlapping of resonances causes the emergence of ray chaos with exponential proliferation of eigenrays. Under chaotic conditions the number of eigenrays contributing to a given mode also grows exponentially with range, giving rise to a very complicated range dependence of mode amplitudes. Numerical simulations presented in Refs. [58, 59] support these statements.

It might be assumed that that exponential proliferation of eigenrays contributing to a given mode leads to statistical independence of mode amplitude fluctuations under chaotic conditions. We expect, however, that the problem of describing mode amplitudes is considerably more rich and complicated. First, it should be recalled that generically the phase space of a chaotic Hamiltonian system contains both chaotic regions and “stable islands” formed by regular periodic trajectories. Some such regular rays will be eigenrays for some modes. Their contributions to modes cannot be considered as stochastic. Thus, we expect that under chaotic conditions there will be modes with amplitudes composed of two constituents: a chaotic one and a regular one. Numerical results illustrating this statement have been presented in Ref. [59]. Another important phenomenon typical of chaotic dynamics, which may affect modal structure variations is stickiness, i.e., the presence of segments of a chaotic trajectory which exhibit almost regular behavior. The interval over which apparently regular behavior is observed can be long. In principle, one can presume that stickiness may cause some long-lasting correlations of mode amplitudes [40].

Our ray-based description of normal mode amplitudes has restrictions that are very much like those of standard ray theory. In particular, at some points the contribution from an eigenray to a given mode can be infinite. This occurs when the derivative in the denominator in Eq. (52) vanishes. (The same comment applies to Eq. (60), below.) Such divergences represent analogs of standard ray theory caustics. Under conditions of ray chaos the number of such caustics grows exponentially with range, spoiling applicability of the ray-based description already at short distances. This issue is discussed in Ref. [59]. On the other hand, in Ref. [59] (see also Ref. [46]) it was demonstrated numerically that the approach considered in this section can properly predict squared mode amplitudes smoothed over the mode number at ranges of order of at least ten inverse

Lyapunov exponents. This result is rather encouraging. It gives us hope that energy redistribution between modes can be comparatively easily analyzed using simple ray calculations at ranges of the order of a few thousand km.

So far, we have considered only a cw field. For a signal with a finite bandwidth, the mode sum must include an integration over frequency σ . The pulse signal at the point (z, r) can be represented as

$$u(z, r, t) = \sum_m u_m(z, r, t), \quad (57)$$

where

$$u_m(z, r, t) = \int d\sigma s(\sigma) B_m(r, \sigma) \psi_m(z, \sigma) e^{i\sigma\left(\frac{r}{c_0} - t\right)} \quad (58)$$

with $s(\sigma)$ being the spectrum of the initially radiated pulse. In Eq. (58) we indicate explicitly the dependencies of B_m and ψ_m on σ which have been omitted until now. Each term, $u_m(z, r, t)$, in the sum (57) can be interpreted as a pulse carried by an individual mode and we shall call it the “mode” pulse. The mode pulse, in turn, can be regarded as a superposition of elementary pulses representing contributions from different terms in the sum (52):

$$u_m(z, r, t) = \sum_n \int d\sigma s(\sigma) G_m(z, r, \sigma) e^{i\sigma\left(\frac{\Phi_n + r}{c_0} - t\right)}, \quad (59)$$

where

$$G_m(z, r, \sigma) = \frac{e^{i\beta_n}}{\sqrt{k_0 r |\partial I / \partial p_0|_{p_0=p_{0n}}}} \frac{2 \cos\left(k_0 \int_z^z dz' \sqrt{2[E_m - U_0(z')] - \pi/4}\right)}{\sqrt{R_m} [2(E_m - U_0(z))]^{1/4}}. \quad (60)$$

The above expressions depend on mode parameters with the subscript m and eigenrays parameters with the subscript n . Note that both types of parameters depend on frequency. Although the trajectories of eigenrays contributing to the given mode obey frequency-independent Hamilton equations (9), their starting momenta determined by Eq. (50) depend on the eigenvalue I_m . But the latter, according to Eq. (46), does depend on frequency. Under chaotic conditions the number of terms in Eq. (59) can be huge leading to a very complicated shape of the mode pulse.

The expectation that mode pulses are very complicated under chaotic conditions is consistent with the numerical results in Ref. [63], where broadband parabolic-equation simulations of sound transmission through a deep water acoustic waveguide with inhomogeneities induced by random internal waves are described. It was shown that, due to mode coupling, mode pulses were several times longer than was the case in the background range-independent environment, and acquired irregular shapes. In contrast, from the ray perspective, the same weak inhomogeneities caused steep eigenrays to split into clusters of eigenrays (micromultipaths) whose travel time spreads were small and whose centroid had a travel time that was close to that of the eigenray in the background environment. (Recall also section II of the present paper.) The authors of Ref. [63] concluded that “while the high modes may be strongly affected by internal waves they are coherent enough that when they are synthesized together localized wave front results.” A qualitative explanation of this phenomenon has been offered in Ref. [64]. In that paper it was shown that mode pulses may be considerably distorted due to mode coupling already at ranges so short that chaotic ray dynamics has not yet had a chance to reveal itself and every mode is formed by contributions from only two eigenrays. It was also demonstrated how distorted pulses carried by individual modes can combine to produce much less distorted ray-like pulses at the receiver.

Although the mode coupling relations presented above are not easy to test experimentally, we emphasize that these results are important because of the insight they provide into the underlying

propagation physics. In this regard, it should be noted that the mode coupling relations presented above directly address the connection between ray chaos and finite frequency propagation effects, i.e., the wave chaos problem.

VI. DISCUSSION

In this paper we have reviewed results relating to ray dynamics in ocean acoustics. All of these results are intimately linked to the Hamiltonian structure of the ray equations. Most previous studies have emphasized the applicability of KAM theory to oceans with periodic range-dependence and the extreme sensitivity of individual chaotic ray trajectories. To complement these ideas, considerable attention has been focussed on oceans with nonperiodic range-dependence, and we have discussed some forms of stability of distributions of chaotic rays. Also, we have discussed subjects such as nondegeneracy violation, ray intensity statistics and the connection between ray chaos and mode coupling that either haven't, or have only recently, been explored in an underwater acoustic context.

Although our understanding of ray dynamics is currently incomplete, it should be clear that the most pressing problem in this context is to better understand the connection between the ray dynamics and the corresponding finite frequency wavefields. For example, even the seemingly simple task of translating ray intensity statistics to wavefield intensity statistics is complicated by the necessity of making an additional assumption about relative phases and correcting for diffractive effects.

It is our hope that the theoretical results presented in this paper provide a foundation for the analysis of measurements of sound fields at long range in the deep ocean. An analysis of this type will be presented in a forthcoming paper. Our long-term goal of developing tools that can be used to assist in the analysis of measurements accounts, in large part, for the considerable attention that we have devoted to ocean structures with nonperiodic range-dependence.

The ideas and results that we have discussed differ in some important respects from more commonly applied ideas and results associated with the study of wave propagation in random media (WPRM). For example, most long-range underwater acoustic propagation WPRM theories (see, e.g., [65]) assume that stochasticity is caused exclusively by internal waves. From the deterministic chaos point of view, this assumption is difficult to justify inasmuch as non-internal-wave (e.g., mesoscale) structure may excite ray-medium resonances and chaos. Also, in the deterministic chaos point of view, the excitation of ray-medium resonances generally leads to a mixed phase space. Most approaches to WPRM, on the other hand, invoke the assumption that the perturbation to the background sound speed structure is delta-correlated; this leads to stochasticity, but not to a mixed phase space. These topics will be discussed in more detail in future work.

Finally, we wish to remark that the importance of ray methods is not diminished by recent advances, both theoretical and computational, in the development of full wave models, such as those based on parabolic equations. The latter are indispensable computational tools in many applications. In contrast, the principal virtue of ray methods is that they provide insight into the underlying wave physics that is difficult, if not impossible, to obtain by any other means. For this reason ray methods remain important.

ACKNOWLEDGMENTS

We thank F. Tappert for the benefit of discussions on many of the topics included in this paper. This work was supported by Code 321 OA of the U.S. Office of Naval Research.

References

- [1] S. S. Abdullaev and G. M. Zaslavsky, “Stochastic instability of rays and the spekle structure of the field in inhomogeneous media,” *Zh. Eksp. Teor. Fiz.* **87**, 763-775 (1984) [Engl. transl.: *Sov. Phys. JETP* **60**, 435-441 (1985)].
- [2] D. R. Palmer, M. G. Brown, F. D. Tappert and H. F. Bezdek, “Classical chaos in nonseparable wave propagation problems,” *Geophys. Res. Lett.* **15**, 569-572 (1988).
- [3] S. S. Abdullaev and G. M. Zaslavsky, “Fractals and ray dynamics in longitudinally inhomogeneous media,” *Sov. Phys. Acoust.* **34**, 334-336 (1989).
- [4] S. S. Abdullaev and G. M. Zaslavskii, “Classical nonlinear dynamics and chaos of rays in wave propagation problems in inhomogeneous media,” *Usp. Phys. Nauk* **161**, 1-43 (1991).
- [5] M. G. Brown, F. D. Tappert and G. Goñi, “An investigation of sound ray dynamics in the ocean volume using an area-preserving mapping,” *Wave Motion* **14**, 93-99 (1991).
- [6] F. D. Tappert, M. G. Brown and G. Goñi, “Weak chaos in an area-preserving mapping for sound ray propagation,” *Phys. Lett. A* **153**, 181-185 (1991).
- [7] M. G. Brown, F. D. Tappert, G. Goñi and K. B. Smith, “Chaos in underwater acoustics,” in *Ocean Variability and Acoustic Propagation*, edited by J. Potter and A. Warn-Varnas (Kluwer Academic, Dordrecht, 1991), 139-160.
- [8] D. R. Palmer, T. M. Georges and R. M. Jones, “Classical chaos and the sensitivity of the acoustic field to small-scale ocean structure,” *Comput. Phys. Commun.* **65**, 219-223 (1991).
- [9] K. B. Smith, M. G. Brown and F. D. Tappert, “Ray chaos in underwater acoustics,” *J. Acoust. Soc. Am.* **91**, 1939-1949 (1992).
- [10] K. B. Smith, M. G. Brown and F. D. Tappert, “Acoustic ray chaos induced by mesoscale ocean structure,” *J. Acoust. Soc. Am.* **91**, 1950-1959 (1992).
- [11] S. S. Abdullaev, *Chaos and Dynamics of Rays in Waveguide Media*, Edited by G. Zaslavsky (Gordon and Breach science publishers, 1993).
- [12] F. D. Tappert and X. Tang, “Ray chaos and eigenrays,” *J. Acoust. Soc. Am.* **99**, 185-195 (1996).
- [13] G. M. Zaslavsky and S. S. Abdullaev, “Chaotic transmission of waves and ‘cooling’ of signals,” *Chaos* **7**, 182-186 (1997).
- [14] J. Simmen, S. M. Flatté and G.-Yu Wang, “Wavefront folding, chaos and diffraction for sound propagation through ocean internal waves,” *J. Acoust. Soc. Am.* **102**, 239-255 (1997).
- [15] M. Wiercigroch, M. Badiéy, J. Simmen and A. H.-D. Cheng. “Nonlinear dynamics of underwater acoustics,” *J. Sound Vibr.* **220**, 771-786 (1999).
- [16] M. A. Wolfson and F. D. Tappert, “Study of horizontal multipaths and ray chaos due to ocean mesoscale structure,” *J. Acoust. Soc. Am.* **107**, 154-162 (2000).
- [17] M. A. Wolfson and S. Tomsovic, “On the stability of long-range sound propagation through a structured ocean,” *J. Acoust. Soc. Am.* **109**, 2693 (2001).

- [18] L. D. Landau, E. M. Lifshits, *Mechanics* (Nauka, Moscow, 1973).
- [19] B. V. Chirikov, "A universal instability of many-dimensional oscillator systems," *Physics Reports* **52**, 263-379 (1979).
- [20] G. M. Zaslavsky and B. V. Chirikov, "Stochastic instability of non-linear oscillations," *Sov. Phys. Usp.* **14**, 549-672 (1972).
- [21] A. G. Lichtenberg and M. A. Leiberman, *Regular and Stochastic Motion* (Springer Verlag, New York, 1983).
- [22] M. Tabor, *Chaos and Integrability in Nonlinear Dynamics* (Wiley-Interscience, New York, 1989).
- [23] M. G. Brown, "Phase space structure and fractal trajectories in 1 1/2 degree of freedom Hamiltonian systems whose time dependence is quasiperiodic," *Nonlinear Processes in Geophys.* **5**, 69-74 (1998).
- [24] J. A. Colosi and M. G. Brown, "Efficient numerical simulation of stochastic internal-wave-induced sound speed perturbation fields," *J. Acoust. Soc. Am.* **103**, 2232-2235 (1998).
- [25] G. M. Zaslavsky, M. Edelman and B. A. Niyazov, "Self-similarity, renormalization and phase nonuniformity of Hamiltonian chaotic dynamics," *Chaos* **7**, 151-181 (1997).
- [26] E. Ott, *Chaos in Dynamical Systems* (Cambridge University Press, Cambridge, 1993).
- [27] P. Gaspard and G. Nicolis, "Transport Properties, Lyapunov exponents, and Entropy per Unit Time," *Phys. Rev. Lett.* **65**, 1693-1696 (1990).
- [28] N. R. Cerruti and S. Tomsovic, "Sensitivity of wave field evolution and manifold stability in chaotic systems," submitted to *Phys. Rev. Lett.* (2001); nlin.CD/0108016.
- [29] G. M. Zaslavsky, *Physics of Chaos in Hamiltonian Systems* (Imperial College Press, London, 1998).
- [30] A. A. Chernikov, R. Z. Sagdeev and G. M. Zaslavsky, "Chaos: How regular can it be?," *Physics Today* **41**, 27-35 (1988).
- [31] W. H. Munk, "Sound channel in an exponentially stratified ocean with application to SOFAR," *J. Acoust. Soc. Am.* **55**, 220-226 (1974).
- [32] G. Hasinger, R. Giacconi, J.E. Gunn, I. Lehmann, M. Schmidt, D. P. Schneider, J. Trümper, J. Wambsganss, D. Woods, and G. Zamorani, "The ROSAT Deep Survey IV. A distant lensing cluster of galaxies with a bright arc," *Astron. Astrophys.* **340**, L27-L30 (1998).
- [33] *Mesoscopic Quantum Physics*, Eds. E. Akkermans, G. Montambaux, J.-L. Pichard, and J. Zinn-Justin, Les Houches Session LXI, 1994 (Elsevier Science Publishers B.V., Amsterdam, 1995).
- [34] M. A. Topinka, B. J. LeRoy, R. M. Westervelt, S. E. J. Shaw, R. Fleischmann, E. J. Heller, K. D. Maranowski, and A. C. Gossard, "Coherent branched flow in a two-dimensional electron gas," *Nature* **410**, 183 (2001)

- [35] V. I. Shishov, "Theory of wave propagation in random media," *Izvestiya VUZ. Radiofizika* **11**, 866-875 (1968).
- [36] M. V. Berry, "Focusing and twinkling: critical exponents from catastrophes in non-Gaussian random short waves," *J. Phys. A. Math. Gen.* **10**, 2061-2081 (1977).
- [37] J. G. Walker, M. V. Berry and C. Upstill, "Measurements of twinkling exponents of light focused by randomly rippling water," *Optica Acta* **30**, 1001-1010 (1983).
- [38] J. H. Hannay, "Intensity fluctuations beyond a one-dimensional random refracting screen in the short-wavelength limit," *Optica Acta* **29**, 1631-1649 (1982).
- [39] E. J. Heller and S. Tomsovic, "Postmodern Quantum Mechanics," *Physics Today* **46** (7), 38-45 (1993).
- [40] B. Sundaram and G. M. Zaslavsky, "Wave analysis of ray chaos in underwater acoustics," *Chaos* **9**, 483-492 (1999).
- [41] *Quantum chaos: between order and disorder: a selection of papers*, edited by G. Casati and B. V. Chirikov (Cambridge University Press, New York, 1995).
- [42] *Chaos and Quantum Physics*, Eds. M.J. Giannoni, A. Voros, and J. Zinn-Justin, Les Houches Session LII, 1989 (Elsevier Science Publishers B.V., Amsterdam, 1991).
- [43] G. M. Zaslavsky, "Stochasticity in quantum systems," *Phys. Rep.* **80**, 157-250 (1980).
- [44] N. L. Balazs and B. K. Jennings, "Wigner function and other distribution functions in mock phase spaces," *Phys. Rep.* **104**, 347-391 (1984).
- [45] D. Bambusi, S. Graffi and T. Paul, "Long time semiclassical approximation of quantum flows: A proof of the Ehrenfest time," *Asymptotic Analysis* **21**, 149-160 (1999).
- [46] A. L. Virovlyansky and G. M. Zaslavsky, "Evaluation of the smoothed interference pattern under conditions of ray chaos," *Chaos* **10**, 211-223 (2000).
- [47] P. W. O'Connor, S. Tomsovic, and E. J. Heller, "Semiclassical Dynamics in the Strongly Chaotic Regime: Breaking the Log Time Barrier", *Physica D* **55**, 340 (1992).
- [48] M.-A. Sepulveda, S. Tomsovic and E. J. Heller, "Semiclassical propagation: How long can it last?," *Phys. Rev. Lett.* **69**, 402-405 (1992).
- [49] S. Tomsovic and E. J. Heller, "Long-time semiclassical dynamics of chaos: The stadium billiard," *Phys. Rev. E* **47**, 282-299 (1993).
- [50] M. D. Collins and J. F. Lingeitch, "Secular behavior and breakdown of chaotic ray solutions," *IEEE J. Oceanic Eng* **22**, 102-109 (1997).
- [51] M. G. Brown and M. A. Wolfson, "A numerical investigation of semiclassical breakdown in an idealized random medium," in preparation (2001).
- [52] L. B. Felsen, "Hybrid ray-mode fields in inhomogeneous waveguides and ducts," *J. Acoust. Soc. Am.* **62**, 352-361 (1981).
- [53] T. Gao and E. C. Shang, "The transformation between the mode representation and the generalized ray representation of a sound field," *J. Sound Vibr.* **80**, 105-115 (1982).

- [54] L. M. Brekhovskikh and Yu. Lysanov, *Fundamentals of Ocean Acoustics* (Springer-Verlag, Berlin, 1991).
- [55] A. L. Virovlyansky, V. V. Kurin, N. V. Pronchatov-Rubtsov and S. I. Simdyankin, “Fresnel zones for modes,” *J. Acoust. Soc. Am.* **101**, 163-173 (1997).
- [56] A. L. Virovlyanskii and A. G. Kosterin, “Method of smooth perturbations for the description of the fields in multimode waveguides,” *Sov. Phys. Acoust.* **33**, 351-354 (1987).
- [57] A. L. Virovlyansky, A. G. Kosterin and A. N. Malakhov, “Fresnel zones for modes and analysis of field fluctuations in random multimode waveguides,” *Waves in Random Media* **1**, 409-418 (1991).
- [58] A. L. Virovlyansky and G. M. Zaslavsky, “Wave chaos in terms of normal modes,” *Phys. Rev. E.* **59**, 1656-1668 (1999).
- [59] A. L. Virovlyansky, “Manifestation of ray stochastic behavior in a modal structure of the wave field,” *J. Acoust. Soc. Am.* **108**, 84-95 (2000).
- [60] L. D. Landau, E. M. Lifshits, *Quantum Mechanics* (Moscow, Nauka, 1974).
- [61] F. B. Jensen, W. A. Kuperman, M. B. Porter and H. Schmidt, *Computational Ocean Acoustics* (American Institute of Physics, New York, 1994).
- [62] G. P. Berman and G. M. Zaslavsky, “Condition of stochasticity in quantum nonlinear systems,” *Physica A* **97**, 367-382 (1979).
- [63] J. A. Colosi and S. M. Flatté, “Mode coupling by internal waves for multimegameter acoustic propagation in the ocean,” *J. Acoust. Soc. Am.* **100**, 3607-3620 (1996).
- [64] A. L. Virovlyansky, “Comments on ‘Mode coupling by internal waves for multimegameter acoustic propagation in the ocean’[*J. Acoust. Soc. Am.* **100**(6), 3607-3620 (1996)],” *J. Acoust. Soc. Am.* **106**, 1174-1176 (1999).
- [65] S. Flatté, R. Dashen, W. Munk, K. Watson and F. Zachariassen, *Sound Transmission through a Fluctuating Ocean* (Cambridge University Press, Cambridge, 1979).